ELECTROMOTION 2009 – EPE Chapter 'Electric Drives' Joint Symposium, 1-3 July 2009, Lille, France

A Novel DC Voltage Regulation Scheme for Dual-Inverter Grid-Connected Photovoltaic Plants

G. Grandi, D. Ostojic and D. Casadei

Department of Electrical Engineering
University of Bologna, Italy

***Abstract*—A multilevel power conversion scheme for three-phase grid-connected photovoltaic (PV) generation systems is considered in this paper. The scheme is based on two insulated strings of PV panels, each one feeding the dc bus of a standard two-level three-phase voltage source inverter (VSI). Inverters are connected to the grid by a three-phase transformer having open-end windings on inverters side. The resulting conversion structure performs as a multilevel power active filter, doubling the power capability of a single VSI with given voltage and current ratings. The multilevel voltage waveforms are generated by an improved space vector modulation, suitable for the implementation in industrial DSPs. A novel control scheme is proposed to regulate the two dc-link voltages of the multilevel converter according with the requirement of a MPPT algorithm. The whole generation system has been verified by experimental tests with reference to different operating conditions.**

I. Introduction

Because of constantly growing energy demand, grid-connected photovoltaic systems are becoming more and more popular, and many countries have permitted, encouraged, and even funded distributed power generation systems. The technology still has shortcomings such as high initial installation cost and low energy conversion efficiency, thus requiring continuous improvements of both cell and power converter technologies [1]-[3].

The connection of the PV field to the ac grid is usually made with a voltage source inverter, and it may include intermediate dc/dc chopper, transformer, or even both. In many countries the national electric standards require a transformer to achieve galvanic insulation of panels with respect to the grid. The presence of a dc/dc chopper allows the PV panels to operate over a wider voltage range, with a fixed inverter dc voltage and a simplified system design. On the other hand, the dc/dc chopper increases the cost and decreases the conversion efficiency. Transformerless and high-frequency transformer topologies are preferred for avoiding bulky LF transformer, but are usually limited to single-phase connections with powers up to few kW. Hence, PV conversion schemes including a line-frequency transformer prevails in higher power, three-phase systems, ranging from few tens of kW up to MW.

The novel topology for PV grid-connected systems proposed by the Authors in [4], [5] (Fig. 1) has been recently implemented and the experimental results are given in this paper. The conversion system utilizes a dual inverter structure connected to open-end primary windings of a standard three-phase transformer. The whole PV field is shared into two equal PV strings. Each inverter can be directly supplied by a PV string, as shown in Fig. 1, or through dc/dc chopper, an option available for all PV converters. The secondary windings of the transformer can be connected to the grid either with star or delta configuration. Note that the transformer contributes with its leakage inductance to the ac-link inductance required for coupling a VSI with the grid. Furthermore, the presence of a low-frequency transformer enable voltage adaptation, allowing the direct connection of high power generation systems to either low- or medium-voltage grids (10 kV or more).

The resulting three-phase converter is able to operate as a multilevel voltage inverter, equivalent to a three-level inverter, with reduced harmonic distortion and lower *dv/dt* in the output voltages. The main advantage of this topology is the simplified hardware structure with respect to traditional three-level inverters. In fact, standard six-transistor configurations can be readily utilized, without additional circuitry. Besides power generation, the system can operate as an active filter, with additional features such as load balancing, harmonics compensation and reactive power injection.

A novel control scheme is proposed to regulate the dc-link voltage of each VSI, in order to accomplish the voltage requirements of the MPPT controller of the whole PV field. As a first task, the dc voltage regulator acts in order to keep the average value of the two dc-link voltages close to the reference value, given by the MPPT controller. The second task for the voltage regulator is to balance the two dc-link voltages, leading to the same value for both. This task requires the possibility to regulate the power sharing between the two inverters by changing their voltage contribution in total output voltage [6].

II. Dual Inverter Topology

Three-level inverters are a good tradeoff solution between performance and cost in multilevel converters for both medium and high-power applications. The main advantages of three-level inverters over the standard two-level ones are: reduced voltage ratings for the switches, good harmonic spectrum (making possible the use of smaller and less expensive filters). In particular, the waveform of the converter output phase voltage has up to nine levels. However, the control complexity increases

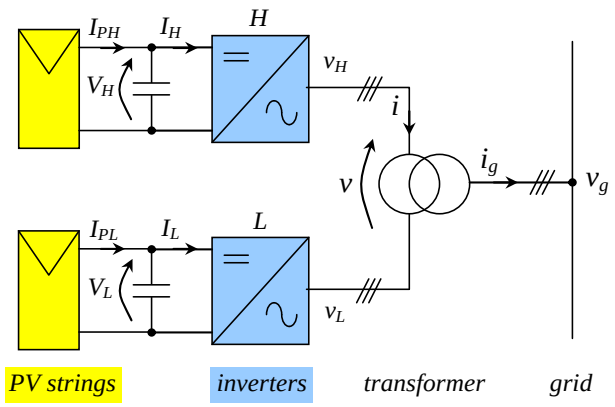

Fig. 1. PV generation system with the dual-inverter configuration.

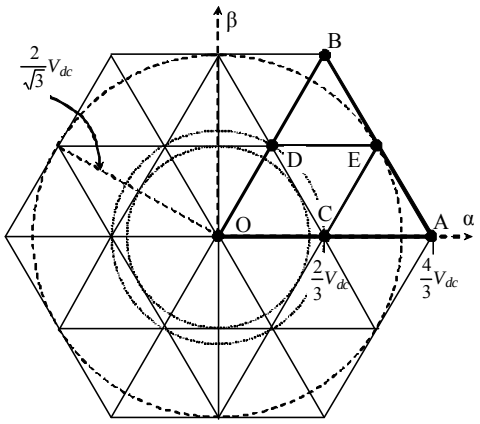

Fig. 2. Dual inverter voltage vector plot in the case $V_H = V_L = V_{dc}$.

compared to conventional voltage-source inverters (VSI). The dual two-level inverter structure (Fig. 1) gives the same output voltage as three-level inverter with a simple combination of standard three-phase VSI [7], [8]. Then, it represents a viable solution when the three-phase output can be connected in the open-winding configuration, as for transformers and ac motors, and especially when the dc source can be easily split in two insulated parts, as for batteries and PV panels. The presence of two insulated dc sources inherently prevents the circulation of common-mode currents, avoiding the use of an additional three-phase common mode reactor. Note that the application of modified voltage modulation algorithms which don't produce common-mode voltages leads to the drawback of lower dc bus voltage utilization [9].

In the present case of PV applications, the required dc voltage level can be obtained by adjusting the number of series-connected panels. The MPPT action is directly performed by the inverters, regulating the dc-bus voltages, as explained in the following section.

With reference to the scheme of Fig. 1, using space vector representation, the output voltage vector $\bar{v}$ of the multilevel converter is given by the sum of the voltage vectors $\bar{v}_H$ and $\bar{v}_L$ generated by inverter H and L, respectively,

$$\bar{v} = \bar{v}_H + \bar{v}_L , \tag{1}$$

being

$$\bar{v}_H = \frac{2}{3} V_H \left(S_{1H} + S_{2H}\, e^{j\frac{2}{3}\pi} + S_{3H}\, e^{j\frac{4}{3}\pi} \right),$$
$$\bar{v}_L = -\frac{2}{3} V_L \left(S_{1L} + S_{2L}\, e^{j\frac{2}{3}\pi} + S_{3L}\, e^{j\frac{4}{3}\pi} \right), \tag{2}$$

where $\{S_{1H}, S_{2H}, S_{3H}, S_{1L}, S_{2L}, S_{3L}\} = \{0, 1\}$ are the switch states of the inverter legs. The combination of the eight switching configuration for each three-phase inverter yields to 64 possible switching states. In the case of $V_H = V_L = V_{dc}$ these switching states correspond to only 19 different output voltage vectors, including zero vector, as represented in Fig. 2. The redundancy of switching states represents a degree of freedom which is useful to develop different modulation strategies.

III. Converter Control

The PV conversion system is based on a symmetric structure, having two inverters with the same voltage and current ratings which are supplied by two equal strings of PV panels. Although the dc bus voltage reference V_{dc}^* is the same for both inverters, to meet demands of the MPPT algorithm, both dc bus voltages V_H and V_L must be regulated to guarantee the system stability for any operating condition. A novel control scheme system is presented in this paper according to the block diagram of Fig. 3. In particular, the voltage controller is described in more detail, whereas the MPPT and other necessary supervisory tasks are not discussed further.

It is worth noting that the control algorithm for the proposed dual-inverter is more complex than that for a single inverter. In fact, for single inverter configuration, the only variable being controlled is ac current whereas, in case of dual inverter, ac voltages sharing between two inverters "H" and "L" must be controlled as well. This additional degree of freedom has been addressed in this paper by a simple combination of proportional-integral (PI) controllers. A more complex solution has been previously proposed by the Authors in [4], [5] with a connection to power sharing problem already addressed in [9] for electric/hybrid traction system based on the same dual inverter configuration. In [10] a multivariable linear quadratic regulator (LQR) based on state-space models was proposed. It has been applied to the equivalent problem of dc-link neutral-point voltage regulation of a three-level neutral-point-clamped (NPC) inverter. Another possibility is the independent control of each inverter, but at the price of loss of proper multilevel waveform [11].

With reference to Fig. 3, the two dc voltages (V_H, V_L) are controlled by two PI controllers, here called "average" and "balance". The average controller acts in order to regulate the average value of dc bus voltages, whereas the balance controller acts in order to equalize the dc bus voltages. The input signals of voltage controllers can be built by adding and subtracting one from the other the voltage errors:

$$\Delta V_L + \Delta V_H = 2\left[\frac{(V_H + V_L)}{2} - V_{dc}^*\right], \tag{3}$$

$$\Delta V_L - \Delta V_H = V_L - V_H, \tag{4}$$

where ΔV_L and ΔV_H are the voltage error signals:

$$\begin{cases} \Delta V_L = V_L - V_{dc}^* \\ \Delta V_H = V_H - V_{dc}^* \end{cases}. \tag{5}$$

The average controller generates the active current reference for the dual inverter, I^*, corresponding to the active power injected into the grid, without taking into account the power sharing between the two inverters "H" and "L". If the current is injected in phase with the grid voltage, the resulting current space vector reference $\bar{i}^*$ is

$$\bar{i}^* = I^* \hat{v}_g, \tag{6}$$

being $\hat{v}_g$ the unity space vector of the grid voltage. It can be noted that reactive and/or harmonic compensation current references can be added to $\bar{i}^*$ if active power filter operation is required.

To solve the known problem of current control in grid-connected application [12], a simple proportional controller with a feed-forward action (grid voltage) has been adopted, due to its simplicity, good dynamic response and immunity to harmonic disturbance. In particular, the reference voltage $\bar{v}^*$ is calculated as

$$\bar{v}^* = K(\bar{i}^* - \bar{i}) + \bar{v}_g' \tag{7}$$

being $\bar{v}_g'$ the space vector of the grid voltage at the inverter side. Although resonant controllers [13] generally provide better characteristics compared to proportional controllers, this advantage becomes less relevant as the switching frequency increases. The fast response of a proportional controller provides necessary decoupling from the outer voltage control loop, which is much slower due to the significant dc-link capacitance. Furthermore, a small steady-state current error is not a critical drawback in the proposed system, since the controlled variables are dc voltages [4], [5].

The reference output voltage $\bar{v}^*$ calculated by (7) can be synthesized as the sum of the voltages $\bar{v}_H^*$ and $\bar{v}_L^*$ generated by the two inverters, as expressed by (1). In order to equalize the two dc bus voltages V_H and V_L, the balance PI controller determines the power sharing between the two inverters "H" and "L", as shown in Fig. 3. Introducing the voltage ratio k and imposing the inverter voltage vectors $\bar{v}_H^*$ and $\bar{v}_L^*$ to be in phase with the output voltage vector $\bar{v}^*$, yields

$$\begin{cases} \bar{v}_H^* = k\,\bar{v}^* \\ \bar{v}_L^* = (1-k)\,\bar{v}^* \end{cases}. \tag{8}$$

The condition expressed by (8) allows maximum dc voltage utilization. Being the output current of the two inverters the same, the coefficient k also defines the power sharing between the two inverters. In terms of averaged values within the switching period, the output power can be expressed as

$$p = \frac{3}{2}\bar{v}^* \cdot \bar{i} = p_H + p_L \quad \begin{cases} p_H = \frac{3}{2}\bar{v}_H^* \cdot \bar{i} = k\,p \\ p_L = \frac{3}{2}\bar{v}_L^* \cdot \bar{i} = (1-k)\,p \end{cases}. \tag{9}$$

The coefficient k has a limited variation range depending on the value of the reference output voltage $\bar{v}^*$, as already investigated by the Authors in [6].

Furthermore, it has to be verified that both references are within the range of achievable output voltages of each inverter, which depend on their dc voltages. In the case of a single inverter topology, if the voltage demand exceeds available dc voltage, the output voltage is simply saturated. With the dual inverter configuration, total voltage reference must be satisfied, so in case of voltage saturation of one inverter the second has to provide for the missing part. This problem was addressed in [5].

Once the inverter reference voltages $\bar{v}_H^*$ and $\bar{v}_L^*$ are determined by (8), they must be synthesized by the dual two-level inverter and applied to the open-end windings of the transformer. Generally, all pulse-width modulators for dual inverter can be divided in two groups:

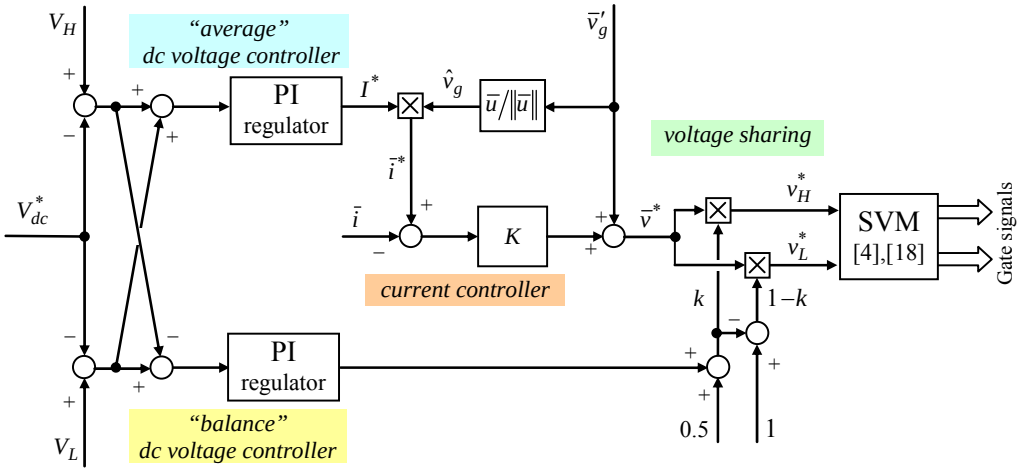

Fig. 3. Block diagram of proposed control system.

- the first group uses two independent modulators for the two single inverters [11], [14]. This approach is characterized by simplicity and large degree of freedom, leading to an independent modulation of $\bar{v}_H$ and $\bar{v}_L$. However, it fails in proper multilevel waveform generation and, consequently, the output voltage includes higher harmonic distortion and the *dv*/*dt* is increased;
- the second group consists of composite modulators, which are able to produce proper multilevel voltage waveforms. As in the case of single inverter, there are carrier-based (CB) and space vector (SV) PWMs. The earliest proposed CB modulation for dual three-phase inverters was sine-sawtooth modulation with carriers phase-shifted by 180° [7]. Another known CB algorithm is a sine-triangle modulation adopted from the "phase opposition disposition" approach of traditional 3-level inverters [15], which can be easily extended to dual inverter configuration. Finally, a space vector PWM has been proposed in [16], where the role of the two inverters is transposed at the end of each switching period in order to obtain a symmetric behavior. All the algorithms of this group can work only with identical reference voltages, i.e., $\bar{v}_H^* = \bar{v}_L^*$, and they cannot provide proper multilevel output voltage in case of different references.

A SVM method developed to overcome these problems has been presented in [9], [17]. However, this method leads to switching sequences that are difficult to be implemented in the sole PWM generation unit of an industrial DSP which usually provides a unique carrier for all three phases. For this reason, the Authors presented a modified SVM algorithm in [18], more suitable for an implementation. It introduces use of asymmetrical PWM in order to avoid application of different carriers, as mentioned above. This algorithm has been considered in this paper and the corresponding experimental results are shown in the next section.

TABLE I
SUMMARY OF THE MAIN PARAMETERS OF THE PV CONVERSION SYSTEM

PV PANELS	
type	Shell Solar SQ150-C
string arrangement (H and L)	6 panels in parallel
connection cables resistance	43 [mΩ]
test condition: irradiance, cell temp.	950 [W/m^2], 58 [°C]
INVERTERS	
configuration (H and L)	two-level VSI
MOSFETs (6 in parallel per switch)	IRF2807
MOSFETs ratings	V_{DSS}=75[V]; R_{DS}=13[mΩ]
dc-bus capacitance	23 [mF]
switching frequency	20 [kHz]
TRANSFORMER and GRID	
turn ratio	230/24 [V/V]
converter/grid-side winding connection	open ends/star
rated power	1500 [VA]
short circuit voltage	6.9 [%]
ac link inductance (converter side)	0.4 [mH]
grid voltage (line-to-line), frequency	350 [V], 50 [Hz]

IV. EXPERIMENTAL RESULTS

A complete PV generation system prototype based on the proposed multilevel converter has been realized. The system supply is based on parallel connection of PV panels with resulting PV string voltage around 30-40 V, allowing to use of low-voltage, high-current MOSFETs. These types of static switches are cheap and have good efficiency, since their on-state resistance is a strong decreasing function of the blocking voltage rating (V_{DSS}). The presence of a grid-transformer with the proper turn ratio enables voltage adaptation. Furthermore, low operating voltages guarantee the electric safety during experiments.

The main characteristics of the whole system are summarized in Table I. Reference is made to the scheme with two PV strings directly connected to the multilevel converter, without intermediate dc/dc choppers, as represented in Fig. 1. In this case, the MPPT regulation is achieved by adjusting the dc bus voltage reference V_{dc}^* of the two inverters.

Each one of the two identical PV strings consists of a parallel arrangement of six "*Solar Shell*" SP150 modules. Four power cables with a length of about 50 m connect the strings from the roof to the Lab of the Department where the inverters are placed. A picture of the twelve PV panels used for the tests is given in Fig. 4(a). The I-V and P-V characteristics of the PV modules, given in Fig. 4(b), are related to the environmental condition during the ex-

(a)

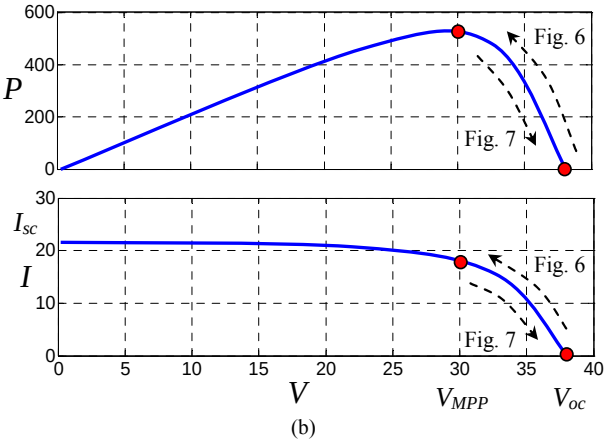

(b)

Fig. 4. PV panels utilized for tests. (a) Picture of the arrangement on the roof. (b) P-V and I-V characteristics of the two PV strings.

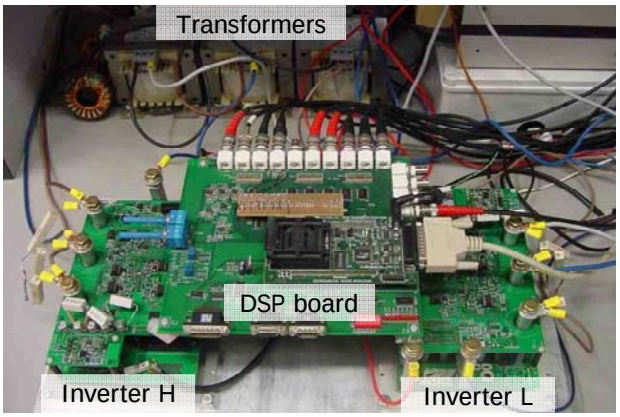

Fig. 5. Experimental set-up

perimental test in terms of solar irradiance and temperature of the module.

The control algorithm presented in Section III has been implemented in TMS320F2812 digital signal processor capable of controlling two three-phase inverters simultaneously. A picture of the hardware arrangement of the multilevel converter prototype is given in Fig. 5.

The experimental tests show the dynamic behavior of the system in response to step changes of the dc voltage reference, V_{dc}*, simulating the action of a MPPT algorithm. The voltage excursion has been chosen to be large enough in order to verify both the dynamic response and the stability of the proposed control system.

In the first case, Fig. 6, the voltage reference decreases from 38 V to 30 V, approximately, corresponding to open-circuit voltage and MPP voltage, respectively (see Fig. 4 (b)). This step leads to a sudden increment of the PV generated power. In particular, Fig. 6 (a) shows the time response of dc voltage and dc current for both the inverters. It can be seen that the system reaches steady-state condition without overshoot in less than 40 ms, meaning only two periods of grid voltage.

The output of the dual inverter (ac voltage and ac current) is shown in Fig. 6 (b). During this transient there is an increase of the modulation index due to the lowering of the dc voltage. As expected, the instantaneous values of the resulting output voltage *v* changes its waveform from seven-level (region between the two smaller circles in Fig. 2) to nine-level (region between the two larger cir-

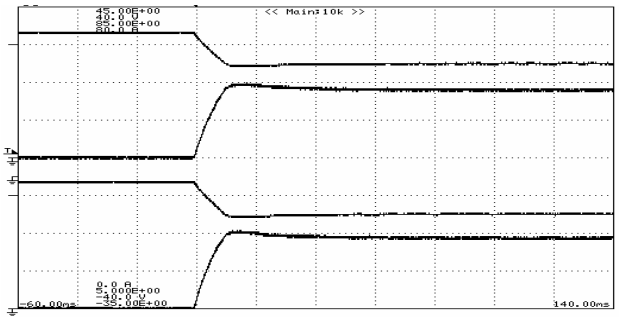

(a) dc voltage (10 V/div, 35 V offset) and dc current (10 A/div) for both inverters, V_H, I_{PH}, V_L, I_{PL} (from top to bottom).

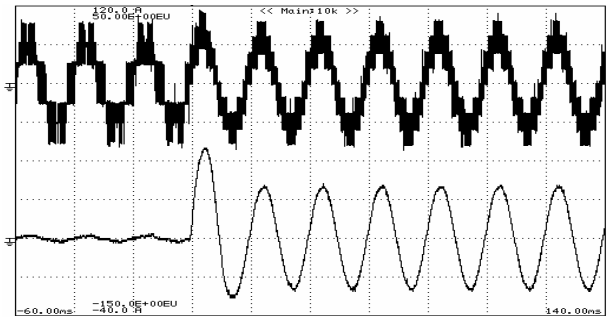

(b) converter ac voltage (20 V/div) and ac current (20 A/div).

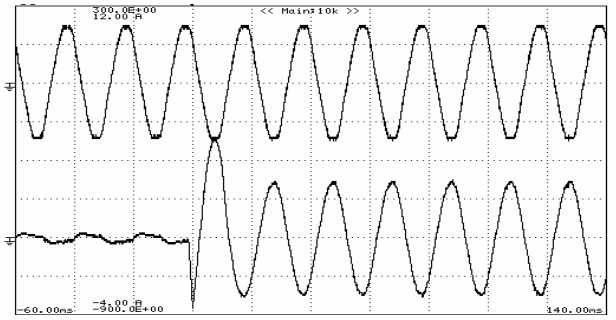

(c) grid voltage (upper, 150 V/div) and grid current (lower, 2 A/div).

Fig. 6. Experiment: step change (decrease) of the reference dc voltage, V_{dc}^*, from 38 V to 30 V, time scale 20ms/div (ref. to Fig. 4).

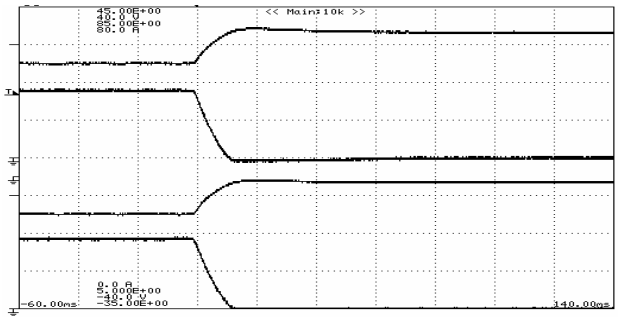

(a) dc voltage (10 V/div, 35 V offset) and dc current (10 A/div) for both inverters, V_H, I_{PH}, V_L, I_{PL} (from top to bottom).

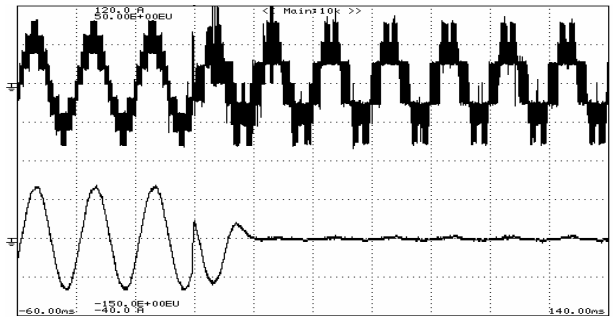

(b) converter ac voltage (20 V/div) and ac current (20 A/div).

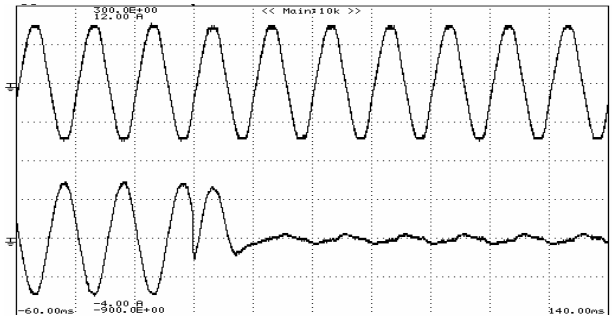

(c) grid voltage (upper, 150 V/div) and grid current (lower, 2 A/div).

Fig. 7. Experiment: step change (increase) of the reference dc voltage, V_{dc}^*, from 30 V to 38 V, time scale 20ms/div (ref. to Fig. 4).

cles in Fig. 2). These results confirm the correct operation of the multilevel modulation technique in these regions. The resulting current ripple practically disappears, as shown in Fig. 6 (b). Fig. 6 (c) shows that grid voltage (line-to-neutral) and grid current are in phase, as expected. Being the grid voltage fixed, the current amplitude increases in response of the sudden change of the PV generated power. It can be noted that, for grid connected application producing only active power, the MPP corresponds to the operating point with maximum grid current amplitude.

The second case, Fig. 7, is related to the opposite step of the voltage reference V_{dc}^{*}, from 30 V to 38 V, yielding to a sudden decrement of PV generated power (see Fig. 4 (b)). Fig. 7 (a) shows the time response of dc voltage and dc current for both the inverters. Also in this case, the system response is good and steady state condition is reached in few ac periods, without overshoot. The output of the dual inverter (ac voltage and ac current) during the transient is shown in Fig. 7 (b). In this case, a decrease of modulation index due to the higher available dc voltage can be noted. Fig. 7 (c) shows grid voltage and grid current. The transient affects only the grid current amplitude, as stated for the previous case.

V. Conclusion

A novel dual inverter control scheme for the grid connection of a photovoltaic generation system has been proposed in this paper. The topology includes two insulated PV strings and a three-phase open-end winding transformer. The power electronic converter consists of a dual three-phase VSI. The resulting output voltages present a multilevel waveform, equivalent to the one of a three-level inverter, but obtained with a simple combination of standard two-level VSI. In this way, the output current ripple practically disappears. Furthermore, the energy generation is provided to the grid with a power factor that approaches unity and additional active filter tasks could be readily introduced. For the generation of the proper multilevel waveforms, a modified SVM algorithm has been adopted, having the merit to be easily implemented in industrial DSP controllers without the need of additional hardware (e.g. FPGA). The regulation of the PV string voltages is directly performed by the inverters by means of a novel voltage controller. The proposed voltage regulation scheme is simple to implement and easy to tune, since it is separated for the inner current control loop. The complexity of the control system compared to the single three-phase inverter has been increased just with an additional PI controller.

The whole PV generation system has been implemented and verified by experimental tests, showing good performance both in steady state and transient operating conditions. In particular, the settling time in response to PV voltage transient is very small, in the order of tens of ms. In this way, demands of MPPT controller due to solar irradiance and/or temperature changes can be easily satisfied.

References

[1] S. Kjaer, J. Pedersen, F. Blaabjerg, "A Review of Single-Phase Grid-Connected Inverters for Photovoltaic Modules," *IEEE Trans. on Industry Applications*, Vol. 41, No. 5, Sep 2005, pp. 1292-1306.

[2] T. Shimizu, M. Hirakata, T. Kamezawa, and H. Watanabe, "Generation control circuit for photovoltaic modules," *IEEE Trans. on Power Electronics*, Vol. 16, No. 3, May 2001, pp. 293-300.

[3] J.-H. Park, J.-Y. Ahn, B.-H. Cho, G.-J. Yu, "Dual-Module-Based Maximum Power Point Tracking Control of Photovoltaic Systems", IEEE *Trans. on Industry Applicat.*, vol. 53, No. 4, June 2006, pp. 1036- 1047.

[4] G. Grandi, D. Ostojic, C. Rossi, "Dual Inverter Configuration for Grid-Connected Photovoltaic Generation Systems," *Proc. 29th Int. Tel. En. Conf., INTELEC*, Sept. 30 –Oct. 4, 2007, Rome, Italy, pp. 880-885.

[5] G. Grandi, D. Ostojic, C. Rossi, D. Casadei, "Multilevel Power Conditioner for Grid-Connected Photovoltaic Applications," *14th IEEE MELECON Conference*, May 5-7, 2008, Ajaccio, France, pp. 573-578.

[6] G. Grandi, C. Rossi, A. Lega, D. Casadei, "Multilevel operation of a dual two-level inverter with power balancing capability," *Proc. of IEEE Industry Applications Soc. Annual Meeting, IEEE-IAS*, Tampa, Florida (USA), Oct. 8 - 12, 2006.

[7] I. Takahashi and Y. Ohmori, "High-performance direct torque control of an induction motor," *IEEE Trans. Industry Applications*, Mar. 1989, vol. 25, no. 2, pp. 257-264.

[8] H. Stemmler and P. Guggenbach, "Configurations of high-power voltage source inverter drives," in *Proc. of European Power Electronics Conference*, EPE 1993, vol. 5, pp. 7-14.

[9] M. Baiju, K. Mohapatra, R. Kanchan, K. Gopakumar, "A dual two-level inverter scheme with common mode voltage elimination for an induction motor drive," *IEEE Trans. on Power Electronics*, vol. 19, No. 3, May 2004, pp. 794-805.

[10] S. Alepuz, S. Busquets-Monge, J. Bordonau, J. Gago, D. Gonzalez, J. Balcells, "Interfacing Renewable Energy Sources to the Utility Grid Using a Three-Level Inverter," *IEEE Trans. on Industrial Electronics*, vol. 53, no. 5, Oct. 2006, pp. 1504-1511.

[11] J. Kim, J, Jung, K, Nam, "Dual-inverter control strategy for high-speed operation of EV induction motors," *IEEE Trans. on Industrial Electronics*, vol. 51, no. 2, Apr. 2004, pp. 312- 320.

[12] F. Blaabjerg, R. Teodorescu, M. Liserre, A.V. Timbus, "Overview of Control and Grid Synchronization for Distributed Power Generation Systems," *Trans. on Industrial Electronics*, vol. 53, no. 5, pp. 1398-1409, Oct. 2006.

[13] M. Liserre, R. Teodorescu, F. Blaabjerg, "Multiple harmonics control for three-phase grid converter systems with the use of PI-RES current controller in a rotating frame", IEEE *Trans. on Power Electronics*, vol. 21, No. 3, May 2006, pp. 836 – 841.

[14] B. Welchko, "A Double-Ended Inverter System for the Combined Propulsion and Energy Management Functions in Hybrid Vehicles with Energy Storage", in *Proc. IEEE 31st Industrial Electronics Ann. Conf.*, Nov. 2005, pp. 1401-1406.

[15] D. Holmes, T. Lipo, *Pulse Width Modulation for Power Converters: Principles and Practice*, Wiley-IEEE Press, 2003, pp. 469–470.

[16] E. G. Shivakumar, K. Gopakumar et al., "Space vector PWM control of dual inverter fed open-end winding induction motor drive," *Proc. of 16th IEEE Applied Power Electronics Conf.*, Anaheim, 2001, pp. 399-405.

[17] C. Rossi, D. Casadei, G. Grandi, A. Lega, "Multilevel Operation and Input Power Balancing for a Dual Two-Level Inverter with Insulated DC Sources", IEEE *Trans. on Industry Applications*, vol. 44, No. 6, Nov/Dec 2008. pp. 1815-1824.

[18] G. Grandi, D. Ostojic, "Dual Inverter Space Vector Modulation with Power Balancing Capability," *IEEE Region 8 Conference EUROCON 2009*, St. Petersburg, Russia, May 2009.